

IEEE JOURNAL OF SELECTED TOPICS IN APPLIED EARTH OBSERVATIONS AND REMOTE SENSING

A PUBLICATION OF THE IEEE GEOSCIENCE AND REMOTE SENSING SOCIETY
AND THE IEEE COMMITTEE ON EARTH OBSERVATIONS



JUNE 2016

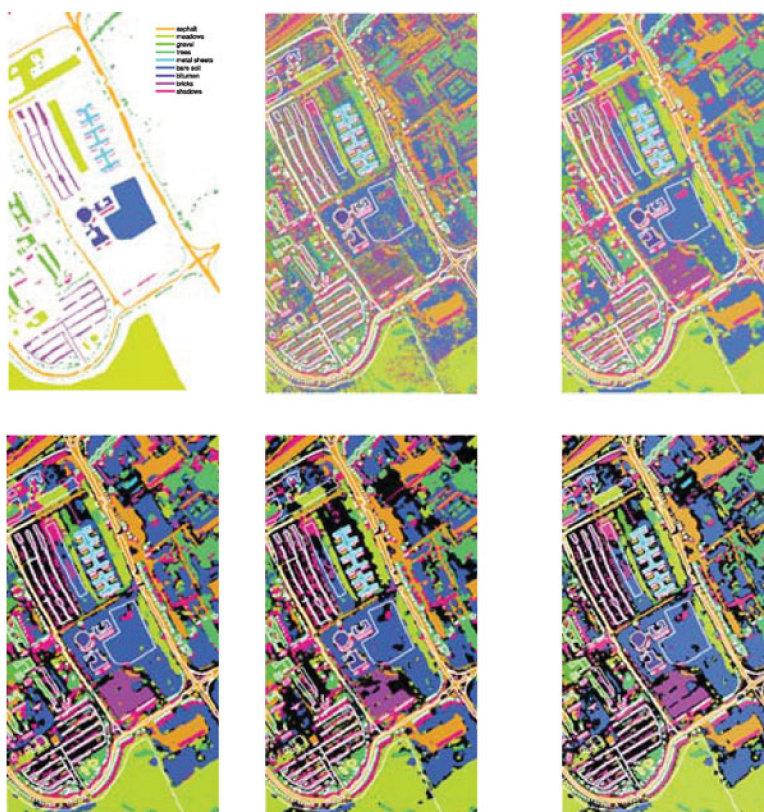
VOLUME 9

NUMBER 6

IJSTHZ

(ISSN 1939-1404)

SPECIAL ISSUE ON 2015 INTERNATIONAL GEOSCIENCE AND REMOTE SENSING SYMPOSIUM



Classification of the Pavia University (Pavia, Italy) scene acquired by the ROSIS sensor: Ground truth (top left) and several classification results with and without context and rejection. For more information, see “Supervised Hyperspectral Image Classification With Rejection,” by Condessa *et al.*, which begins on p. 2321.

IEEE JOURNAL OF SELECTED TOPICS IN APPLIED EARTH OBSERVATIONS AND REMOTE SENSING

A PUBLICATION OF THE IEEE GEOSCIENCE AND REMOTE SENSING SOCIETY
AND THE IEEE COMMITTEE ON EARTH OBSERVATIONS



JUNE 2016

VOLUME 9

NUMBER 6

IJSTHZ

(ISSN 1939-1404)

SPECIAL ISSUE ON 2015 INTERNATIONAL GEOSCIENCE AND REMOTE SENSING SYMPOSIUM

Foreword to the Special Issue on the 2015 IEEE International Geoscience and Remote Sensing Symposium	2101
<i>S. B. Serpico, V. Pascazio, L. Bruzzone, and P. Gamba</i>	
<hr/>	
<i>Processing and Analysis of Radar, SAR, and Seismic Data</i>	
Efficient and Robust RFI Extraction Via Sparse Recovery	2104
<i>L. H. Nguyen and T. D. Tran</i>	
SAR Image Despeckling by Soft Classification	2118
<i>D. Gragnaniello, G. Poggi, G. Scarpa, and L. Verdoliva</i>	
Scattering-Based SARBM3D	2131
<i>G. Di Martino, A. Di Simone, A. Iodice, G. Poggi, D. Riccio, and L. Verdoliva</i>	
An Improved Adaptive Regularization Method for Forward Looking Azimuth Super-Resolution of a Dual-Frequency Polarized Scatterometer	2145
<i>L. Liu, X. Dong, J. Zhu, and D. Zhu</i>	
Ground-Based SAR Wide View Angle Full-Field Imaging Algorithm Based on Keystone Formatting	2160
<i>T. Zeng, C. Mao, C. Hu, and W. Tian</i>	
Experimental Study of Ionospheric Impacts on Geosynchronous SAR using GPS Signals	2171
<i>X. Dong, C. Hu, Y. Tian, W. Tian, Y. Li, and T. Long</i>	
Superresolution Downward-Looking Linear Array Three-Dimensional SAR Imaging Based on Two-Dimensional Compressive Sensing	2184
<i>S. Zhang, G. Dong, and G. Kuang</i>	
Nonsmooth Nonconvex Optimization for Low-Frequency Geosounding Inversion	2197
<i>H. Hidalgo-Silva and E. Gómez-Treviño</i>	
SAR Imagery Feature Extraction Using 2DPCA-Based Two-Dimensional Neighborhood Virtual Points Discriminant Embedding	2206
<i>J. Pei, Y. Huang, W. Huo, J. Wu, J. Yang, and H. Yang</i>	
Land Cover Semantic Annotation Derived from High-Resolution SAR Images	2215
<i>C. O. Dumitru, G. Schwarz, and M. Datcu</i>	
A Modified $H-\alpha$ Classification Method for DCP Compact Polarimetric Mode by Reconstructing Quad H and α Parameters From Dual Ones	2233
<i>S. Ghods, S. V. Shojaedini, and Y. Maghsoudi</i>	
A Sparse Bayesian Imaging Technique for Efficient Recovery of Reservoir Channels With Time-Lapse Seismic Measurements	2242
<i>F. Sana, F. Ravanelli, T. Y. Al-Naffouri, and I. Hoteit</i>	

(Contents Continued on Page 2098)



Image Processing and Analysis

MTF-Based Deblurring Using a Wiener Filter for CS and MRA Pansharpening Methods *F. Palsson, J. R. Sveinsson, M. O. Ulfarsson, and J. A. Benediktsson* 2255

Parallel and Distributed Dimensionality Reduction of Hyperspectral Data on Cloud Computing Architectures *Z. Wu, Y. Li, A. Plaza, J. Li, F. Xiao, and Z. Wei* 2270

Application and Evaluation of a Hierarchical Patch Clustering Method for Remote Sensing Images *W. Yao, O. Loffeld, and M. Datcu* 2279

Producing Subpixel Resolution Thematic Map From Coarse Imagery: MAP Algorithm-Based Super-Resolution Recovery *L. Wang, P. Wang, and C. Zhao* 2290

Spectral-Spatial Classification Based on Affinity Scoring for Hyperspectral Imagery *Z. Chen and B. Wang* 2305

Supervised Hyperspectral Image Classification With Rejection *F. Condessa, J. Bioucas-Dias, and J. Kovačević* 2321

A Hyperheuristic Approach for Unsupervised Land-Cover Classification *J. P. Papa, L. P. Papa, D. R. Pereira, and R. J. Pisani* 2333

Semantic Classification of High-Resolution Remote Sensing Images Based on Mid-level Features *J. Zhang, T. Li, X. Lu, and Z. Cheng* 2343

Coalition Game Theory-Based Feature Subspace Selection for Hyperspectral Classification *P. Gurram, H. Kwon, and C. Davidson* 2354

Hyperspectral Airborne “Viareggio 2013 Trial” Data Collection for Detection Algorithm Assessment *N. Acito, S. Matteoli, A. Rossi, M. Diani, and G. Corsini* 2365

Fusion of Hyperspectral and Multispectral Images Using Spectral Unmixing and Sparse Coding *Z. H. Nezhad, A. Karami, R. Heylen, and P. Scheunders* 2377

Hyperspectral Blind Reconstruction From Random Spectral Projections *G. Martín and J. M. Bioucas-Dias* 2390

Enhancing Hyperspectral Endmember Extraction Using Clustering and Oversegmentation-Based Preprocessing *F. Kowkabi, H. Ghassemian, and A. Keshavarz* 2400

Remote Sensing of the Cryosphere

Landfast First-Year Snow-Covered Sea Ice Reconstruction via Electromagnetic Inversion *N. Firoozy, P. Mojabi, J. Landy, and D. G. Barber* 2414

Firn Stratigraphic Genesis in Early Spring: Evidence From Airborne Radar *B. Feng, D. Braaten, J. Paden, and P. Gogineni* 2429

Ka-Band Mapping and Measurements of Interferometric Penetration of the Greenland Ice Sheets by the GLISTIN Radar *S. Hensley, D. Moller, S. Oveisgharan, T. Michel, and X. Wu* 2436

Antarctic Sea-Ice Classification Based on Conditional Random Fields From RADARSAT-2 Dual-Polarization Satellite Images *T. Zhu, F. Li, G. Heygster, and S. Zhang* 2451

Land Applications

Retrieving Soil Temperature at a Test Site on the Yamal Peninsula Based on the SMOS Brightness Temperature Observations *K. V. Muzalevskiy and Z. Ruzicka* 2468

Robust Assessment of an Operational Algorithm for the Retrieval of Soil Moisture From AMSR-E Data in Central Italy *E. Santi, S. Paloscia, S. Pettinato, L. Brocca, and L. Ciabatta* 2478

SMOS Near-Surface Salinity Stratification Under Rainy Conditions *A. Santos-Garcia, M. M. Jacob, and W. L. Jones* 2493

Parcel-Based Crop Classification in Ukraine Using Landsat-8 Data and Sentinel-1A Data *N. Kussul, G. Lemoine, F. J. Gallego, S. V. Skakun, M. Lavreniuk, and A. Yu. Shelestov* 2500

Paddy-Rice Phenology Classification Based on Machine-Learning Methods Using Multitemporal Co-Polar X-band SAR Images *Ç. Küçük, G. Taşkın, and E. Erten* 2509

L-Band Passive and Active Signatures of Vegetated Soil: Simulations With a Unified Model *L. Guerriero, P. Ferrazzoli, C. Vittucci, R. Rahmoune, M. Aurizzi, and A. Mattioni* 2520

Indirect Measurement of Forest Leaf Area Index Using Path Length Distribution Model and Multispectral Canopy Imager *R. Hu, J. Luo, G. Yan, J. Zou, and X. Mu* 2532

Assimilation of LAI and Dry Biomass Data From Optical and SAR Images Into an Agro-Meteorological Model to Estimate Soybean Yield *J. Betbeder, R. Fieuzal, and F. Baup* 2540

Individual Tree Species Classification From Airborne Multisensor Imagery Using Robust PCA *J. Lee, X. Cai, J. Lellmann, M. Dalponte, Y. Malhi, N. Butt, M. Morecroft, C.-B. Schönlieb, and D. A. Coomes* 2554

(Contents Continued from Page 2098)

Shadow Detection and Removal for Occluded Object Information Recovery in Urban High-Resolution Panchromatic Satellite Images	<i>N. Su, Y. Zhang, S. Tian, Y. Yan, and X. Miao</i>	2568
Extraction of Urban Areas From Polarimetric SAR Imagery	<i>B. Azmedroub, M. Ouarzeddine, and B. Souissi</i>	2583
Urban Area Extraction Using X-Band Fully Polarimetric SAR Imagery	<i>J. Susaki and M. Kishimoto</i>	2592
Compensation for Azimuth Angle or Scale Effect on Building Extraction in Urban Using SAR Scales of Polarization and Coherence	<i>A. Du and Y. Wang</i>	2602
<i>Atmosphere Applications</i>		
Precipitation From the Advanced Microwave Scanning Radiometer 2	<i>P. C. Meyers and R. R. Ferraro</i>	2611
Heavy Rain Forecasting by Model Initialization With LAPS: A Case Study	<i>A. Tiesi, M. M. Miglietta, D. Conte, O. Drofa, S. Davolio, P. Malguzzi, and A. Buzzi</i>	2619
Uncertainty Quantification in Land Surface Hydrologic Modeling: Toward an Integrated Variational Data Assimilation Framework	<i>A. Abdolghafoorian and L. Farhadi</i>	2628
<i>Ocean Applications</i>		
Preliminary Evaluation of Sentinel-1A Wind Speed Retrievals	<i>F. Monaldo, C. Jackson, X. Li, and W. G. Pichel</i>	2638
Wind Fields From C- and X-Band SAR Images at VV Polarization in Coastal Area (Gulf of Oristano, Italy)	<i>S. Zecchetto, F. De Biasio, A. della Valle, G. Quattrocchi, E. Cadau, and A. Cucco</i>	2643
Variability of the East Greenland Current in Fram Strait From Subdaily COSMO-SkyMed X-SAR Imagery	<i>A. Ciappa, F. Britti, L. Cesarano, V. Gentile, and L. Pietranera</i>	2651
Statistical Models of Sea Surface Salinity in the South China Sea Based on SMOS Satellite Data	<i>C. Li, H. Zhao, H. Li, and K. Lv</i>	2658
Joint Interpolation of Multisensor Sea Surface Temperature Fields Using Nonlocal and Statistical Priors	<i>R. Fablet and F. Rousseau</i>	2665
Height Precision of SAR Altimeter and Conventional Radar Altimeter Based on Flight Experimental Data	<i>L. Shi, K. Xu, P. Liu, S. Yang, L. Wang, and X. Yu</i>	2676
A Comparative Study of Operational Vessel Detectors for Maritime Surveillance Using Satellite-Borne Synthetic Aperture Radar	<i>M. Stasolla, J. J. Mallorquí, G. Margarit, C. Santamaria, and N. Walker</i>	2687
<i>Missions, Sensors, and Calibration</i>		
Echo Signal Quality Analysis During HY-2A Radar Altimeter Calibration Campaign Using Reconstructive Transponder	<i>J. Wan, W. Guo, F. Zhao, C. Wang, P. Liu, M. Lin, H. Peng, and C. Xu</i>	2702
Development of the Reconstructive Transponder for In-Orbit Calibration of HY-2A Altimeter	<i>C. Wang, W. Guo, F. Zhao, J. Wan, P. Liu, M. Lin, H. Peng, and C. Xu</i>	2709
Radar Parameter Design for Geosynchronous SAR in Squint Mode and Elliptical Orbit	<i>Z. Ding, W. Yin, T. Zeng, and T. Long</i>	2720
Use of the GPM Constellation for Monitoring Heavy Precipitation Events Over the Mediterranean Region	<i>G. Panegrossi, D. Casella, S. Dietrich, A. C. Marra, P. Sandò, A. Mugnai, L. Baldini, N. Roberto, E. Adirosi, R. Cremonini, R. Bechini, G. Vulpiani, M. Petracca, and F. Porcù</i>	2733
Reliable and Stable Radiometers for Jason-3	<i>F. Maiwald, O. Montes, S. Padmanabhan, D. Michaels, A. Kitiyakara, R. Jarnot, S. T. Brown, D. Dawson, A. Wu, W. Hatch, P. Stek, and T. Gaier</i>	2754
Validation of Aquarius Soil Moisture Products Over the Northwest of Spain: A Comparison With SMOS	<i>A. González-Zamora, N. Sánchez, and J. Martínez-Fernández</i>	2763
Onboard Radar Processor Development for Rapid Response to Natural Hazards	<i>Y. Lou, D. Clark, P. Marks, R. J. Muellerschoen, and C. C. Wang</i>	2770
On the Use of Gaussian Random Processes for Probabilistic Interpolation of CubeSat Data in the Presence of Geolocation Error	<i>W. Ruan, A. B. Milstein, W. Blackwell, and E. L. Miller</i>	2777
<i>Special Theme: Remote Sensing of Natural Disasters</i>		
A Prototype System for Flood Monitoring Based on Flood Forecast Combined With COSMO-SkyMed and Sentinel-1 Data	<i>G. Boni, L. Ferraris, L. Pulvirenti, G. Squicciarino, N. Pierdicca, L. Candela, A. R. Pisani, S. Zoffoli, R. Onori, C. Proietti, and P. Pagliara</i>	2794
Development and Validation of Fire Damage-Severity Indices in the Framework of the PREFER Project	<i>G. Laneve, L. Fusilli, P. Marzialetti, R. De Bonis, G. Bernini, and L. Tampellini</i>	2806

(Contents Continued on Page 2100)

(Contents Continued from Page 2099)

Predicting the Extent of Wildfires Using Remotely Sensed Soil Moisture and Temperature Trends	2818
. <i>D. Chaparro, M. Vall-llossera, M. Piles, A. Camps, C. Rüdiger, and R. Riera-Tatché</i>	
<i>Special Theme: Remote Sensing for Food Security</i>	
Climate-Related Child Undernutrition in the Lake Victoria Basin: An Integrated Spatial Analysis of Health Surveys, NDVI, and Precipitation Data	2830
. <i>D. López-Carr, K. M. Mwenda, N. G. Pricope, P. C. Kyriakidis, M. M. Jankowska, J. Weeks, C. Funk, G. Husak, and J. Michaelsen</i>	

CALL FOR PAPERS	
IEEE JSTARS Calls for Papers IGARSS'16	2836
